Behavioral Prioritization Enhances Working Memory Precision and Neural Population Gain

Aspen H. Yoo[1], Alfredo Bolaños[1], Grace E. Hallenbeck[1], Masih Rahmati[1], Thomas C. Sprague[2], and Clayton E. Curtis[1]

Abstract

■ Humans allocate visual working memory (WM) resource according to behavioral relevance, resulting in more precise memories for more important items. Theoretically, items may be maintained by feature-tuned neural populations, where the relative gain of the populations encoding each item determines precision. To test this hypothesis, we compared the amplitudes of delay period activity in the different parts of retinotopic maps representing each of several WM items, predicting the amplitudes would track behavioral priority. Using fMRI, we scanned participants while they remembered the location of multiple items over a WM delay and then reported the location of one probed item using a memory-guided saccade. Importantly, items were not equally probable to be probed (0.6, 0.3, 0.1, 0.0), which was indicated with a precue. We analyzed fMRI activity in 10 visual field maps in occipital, parietal, and frontal cortex known to be important for visual WM. In early visual cortex, but not association cortex, the amplitude of BOLD activation within voxels corresponding to the retinotopic location of visual WM items increased with the priority of the item. Interestingly, these results were contrasted with a common finding that higher-level brain regions had greater delay period activity, demonstrating a dissociation between the absolute amount of activity in a brain area and the activity of different spatially selective populations within it. These results suggest that the distribution of WM resources according to priority sculpts the relative gains of neural populations that encode items, offering a neural mechanism for how prioritization impacts memory precision. ■

INTRODUCTION

Working memory (WM), the process involved in maintaining task-relevant information over a short period of time, links perception to behavior and is essential for a broad range of higher-level cognitive functions (Süß, Oberauer, Wittmann, Wilhelm, & Schulze, 2002; Engle, Tuholski, Laughlin, & Conway, 1999; Daneman & Carpenter, 1980). Multiple cortical areas are involved in maintaining information in WM. In parietal and frontal areas, maintaining information in WM is characterized by sustained elevated neural activity during the delay period (Curtis, Rao, & D'Esposito, 2004; Rowe, Toni, Josephs, Frackowiak, & Passingham, 2000; Courtney, Petit, Maisog, Ungerleider, & Haxby, 1998; McCarthy et al., 1994; Funahashi, Bruce, & Goldman-Rakic, 1989; Fuster & Alexander, 1971). Furthermore, there is evidence that these brain areas are retinotopically organized (Jerde, Merriam, Riggall, Hedges, & Curtis, 2012; Schluppeck, Curtis, Glimcher, & Heeger, 2006), and voxels tuned to the location of a remembered stimulus show elevated delay period activation compared with those tuned to other locations (Hallenbeck, Sprague, Rahmati, Sreenivasan, & Curtis, 2021; Saber, Pestilli, & Curtis, 2015). Similarly, in retinotopic visual cortex, a location maintained in visual WM can be successfully decoded from delay period activity (Rahmati, Saber, & Curtis, 2018; Sprague, Ester, & Serences, 2014, 2016; Jerde et al., 2012), along with other remembered visual features, like stimulus orientation, shape, motion direction, pattern, and/or color (Christophel, Hebart, & Haynes, 2012; Riggall & Postle, 2012; Harrison & Tong, 2009; Serences, Ester, Vogel, & Awh, 2009; see Christophel, Klink, Spitzer, Roelfsema, & Haynes, 2017, for a review). Interestingly, in these retinotopic regions, activation averaged across all voxels in a region does not typically display the sustained, elevated activation often seen in frontoparietal areas (Christophel et al., 2012; Riggall & Postle, 2012; Harrison & Tong, 2009; Serences et al., 2009; but see Curtis & Sprague, 2021; Hallenbeck et al., 2021; Saber et al., 2015).

However, in these studies, participants maintained only a single item or multiple items of equal importance. In many cases, we need to remember multiple items with differing levels of importance, and thus, it would be beneficial to "prioritize" the representation of the most important information at the cost of a less robust representation of the least important information. Behavioral studies have demonstrated that participants can utilize cues about the relative reward and probe probability of different items in a WM display to flexibly prioritize the representation of the most valuable or likely-to-be-probed items (Yoo, Klyszejko, Curtis, & Ma, 2018; Emrich, Lockhart, & Al-Aidroos, 2017; Bays, 2014; Klyszejko, Rahmati, & Curtis,

[1]New York University, [2]University of California, Santa Barbara

2014). In these studies, participants respond more accurately or precisely when asked to report the higher-priority items when compared with lower-priority items, suggesting that participants encode information in WM with varying levels of precision to accommodate task goals.

One plausible means of representing information in WM with varying levels of importance may be via modulating the strength of neural representations in a neural "priority map," where the relative activation corresponding to different locations in the scene indexes the relative importance of that location (Jerde et al., 2012; Bisley & Goldberg, 2010; Fecteau & Munoz, 2006; Serences & Yantis, 2006; Thompson & Bichot, 2005). Indeed, there is extensive evidence that activation profiles across neural priority maps reflect the relative importance of different items in a display. For example, attention boosts the activity of neural populations with receptive fields that match the attended location, even in the absence of visual stimuli in the attended area (Rahmati et al., 2018; Sprague, Itthipuripat, Vo, & Serences, 2018; Saber et al., 2015; Gouws et al., 2014; Jerde et al., 2012; Buracas & Boynton, 2007; Serences & Yantis, 2007; Nobre et al., 2004; Gandhi, Heeger, & Boynton, 1999; Kastner, Pinsk, De Weerd, Desimone, & Ungerleider, 1999; Somers, Dale, Seiffert, & Tootell, 1999).

Most of these studies examine the neural consequences of prioritized information on the selective attention of one item in a visual display, leaving unexplored how the brain prioritizes information held in WM (in the absence of visual input) and how multiple items are simultaneously represented across these neural priority maps. In this study, we test the hypothesis that activation in neural priority maps will have higher activation for items maintained in WM with higher priority, and this will in turn result in higher precision of WM reports. Furthermore, we hypothesize that any one neural priority map (one retinotopic area) can represent multiple items and their relative priorities through the activation of local populations tuned to each item's location.

In our study, we asked if the response amplitude of neural populations during a WM delay reflected the relative precision with which items were remembered. To answer this question, we collected event-related BOLD fMRI data from participants while they completed a multi-item spatial WM task. In this task, each of the four items were precued with a different probability of being probed for response, resulting in different memory precisions for each item (Yoo et al., 2018). Importantly, unlike previous research, which only investigated the effects of attended versus unattended stimuli, this experimental design allowed us to simultaneously examine the effects of multiple levels of priority on neural amplitude. We used general linear models (GLMs) and population receptive field (pRF) mapping (Mackey, Winawer, & Curtis, 2017; Dumoulin & Wandell, 2008) to estimate delay period activity and location sensitivity, respectively, which allowed us to independently quantify location-specific delay period

activity for neural populations spatially tuned near the location of each item. We tested the prediction that higher-priority items would exhibit higher-delay period BOLD activity at their corresponding retinotopic location in occipital (V1, V2, V3, V3AB), parietal (IPS0, IPS1, IPS2, IPS3), and frontal (iPCS, sPCS) brain areas. Remarkably, we found that this prediction holds in visual areas alone, suggesting prioritization of WM representations modulates neural gain. On the other hand, frontoparietal regions demonstrated clear elevated delay period activity, independent of the behavioral importance of different items. These results represent a dissociation between the absolute activity in a brain area during a memory delay and whether it encodes relative behavioral relevance through modulations of neural gain.

METHODS

Participants

Eleven participants (five men; mean age = 31.9 years, SD = 6.8 years; five authors) participated in this experiment. Participants had normal or corrected-to-normal vision and no history of neurological disorders. Nonauthor participants were naive to the study hypotheses and were paid $30/hr. We obtained informed, written consent from all participants. The study was in accordance with the Declaration of Helsinki and was approved by the institutional review board of New York University.

Task Procedures

We generated stimuli and interfaced with the MRI scanner, button box, and eye tracker using MATLAB software (The MathWorks) and Psychophysics Toolbox 3 (Brainard, 1997; Pelli, 1997). Stimuli were presented using a PROPixx DLP LED projector (VPixx) located outside the scanner room and projected through a waveguide and onto a translucent screen located at the head of the scanner bore. Participants viewed the screen at a total viewing distance of 64 cm through a mirror attached to the head coil. The display was a circular aperture with an approximately 32-dva (degrees of visual angle) diameter. A trigger pulse from the scanner synchronized the onsets of stimulus presentation and image acquisition.

Participants completed a multi-item probabilistic memory-guided saccade task (Figure 1A). The fixation symbol in this experiment was an encircled fixation cross, with four equally spaced concentric arcs within each quadrant. Each trial began with a 100-msec increase in the size of the outer circle of the fixation symbol. This was followed by a 700-msec endogenous precue, which indicated the probe probability of each item. Probe probability was indicated through the number of illuminated arcs: All four arcs turned white in the quadrant corresponding to the 0.6 item, three arcs for the 0.3 item, two arcs for the 0.1 item, and zero arcs for the 0.0 stimulus. These probe
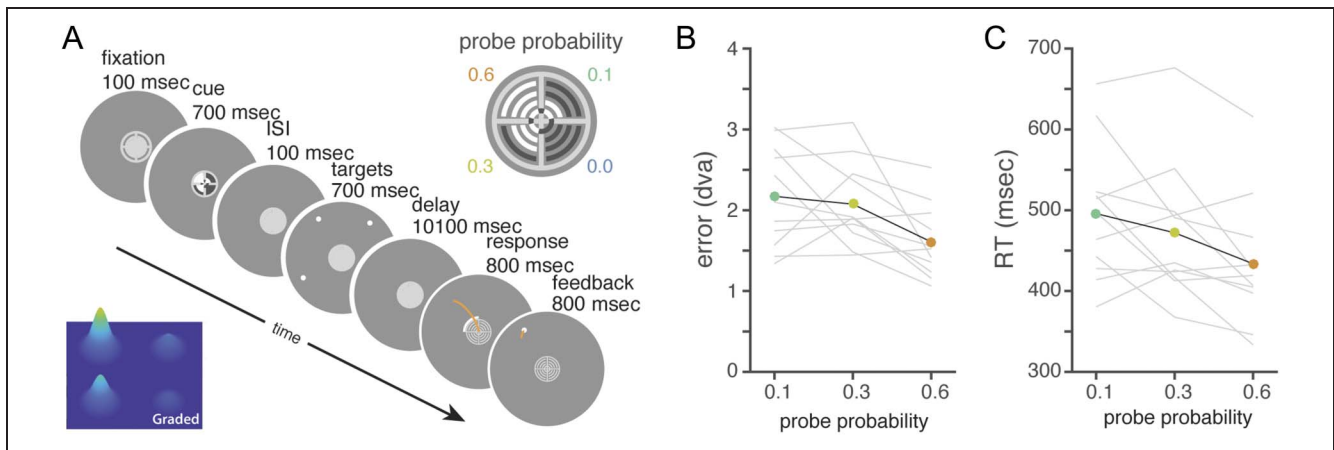
Figure 1. Prioritizing WM representations. (A) Trial sequence. Participants viewed a precue that indicated the probe probabilities of the four targets, each presented in separate visual quadrants, by the number of arcs highlighted within the fixation symbol (top right inset). After the delay, one item was probed for response when a white arc appeared at the outer edge of one quadrant of the fixation symbol. Participants made a memory-guided saccade to the remembered location of the target. The true target location was then presented as feedback, which participants fixated. Bottom left inset: schematic predictions of priority map. Higher priority items will be represented with a taller bump. (B) Memory error (gray: individual participants, black: mean) decreases with increasing priority ($b = -1.16$, $R^2 = .18$, $F = 6.67$, $p = .01$). (C) Memory-guided saccade RT (gray: individual participants, black: mean) decreases with increasing priority ($b = -0.12$, $R^2 = .09$, $F = 3.25$, $p = .08$).

probabilities were veridical across the entire experiment, though not necessarily for each block. The fixation precue had a 0.6-dva radius around the center of the screen. The precue was followed by a 100-msec ISI, then by the items for 700 msec. The items were four white dots, one in each visual quadrant. Items were presented randomly between 9 and 10 dva from fixation. The location of the items in polar coordinates were pseudorandomly sampled from every 10°, avoiding cardinal axes. The item presentation was followed by a 10,100-msec delay. A response cue appeared afterward, which was a white wedge around the quadrant of the fixation symbol corresponding to the probed item. Participants made a memory-guided saccade to the remembered dot location within the corresponding quadrant of the screen. After the saccade, the actual dot location was presented as feedback, and the participant made a corrective saccade to that location. After 800 msec, the feedback disappeared, participants returned their gaze to the central fixation cross, and a variable intertrial interval began. The jittered intertrial interval was pseudo-randomly drawn from three time durations (8800, 10,100, or 11,400 msec) to help deconvolve event-related activity associated with different trial epochs in the fMRI data. Each participant completed one scanning session consisting of 10–14 runs consisting of 12 trials each; they completed a total of 120–168 trials.

Oculomotor Methods

We recorded eye gaze data in the scanner at 1000 Hz (Eyelink 1000, SR Research), beginning with a nine-point calibration and validation scheme. Using our freely available MATLAB iEye toolbox (github.com/clayspacelab/iEye _ts), we transformed raw gaze positions into degrees of visual angle, removed values outside the screen area,

removed artifacts because of blinks, smoothed gaze position with a Gaussian kernel with a standard deviation of 5 msec, and computed the velocity at each time point. Saccadic eye movements were defined with the following criteria: velocity ≥ 30 dva/sec, duration ≥ 8 msec, and amplitude ≥ 0.25 dva. We define RT as the time between the response onset and the initialization of the first saccade and error as the Euclidean distance between the target item and the last saccade landing position. For each trial, data were additionally drift corrected and calibrated to account for measurement noise, such that the gaze position during known trial epochs (i.e., fixation and response period) were at the correct location. Trials were excluded if the participant was not fixating during the delay period, no saccades were found during the response epoch, the initial saccade was too small in amplitude or too long in duration, or the final saccade error was greater than 10°. These exclusion criteria resulted in removing between 4% and 51% ($M = 23.9\%$, $SD = 18.1\%$) of trials per participant. The total trial exclusions were especially high for four participants (42.5%, 42.5%, 47.5%, and 51.3%) because of poor eye-tracking quality, excessive sleepiness, and/or not making saccades during the response period. The exclusion rate of the remaining participants was $M = 11.2\%$, $SD = 5.0\%$. Removing the participants with high exclusion rates do not change the main effects in either the behavioral or neuroimaging results. We therefore retained the usable trials from these participants and performed all analyses with data from all participants.

fMRI Methods

MRI Acquisition

All structural and fMRI data were acquired on a 3-T Siemens Prisma MRI system at the Center for Brain Imaging

at New York University, using the CMRR multiband accelerated EPI pulse sequences (Xu et al., 2013; Feinberg et al., 2010; Moeller et al., 2010). To acquire the functional BOLD contrast images, we used the following settings: multiband 2-D GE-EPI with multiband factor of 4, fifty-six 2-mm interleaved slices with no gap, voxel size = 2 mm, field of view = 208 × 208 mm, no in-plane acceleration, repetition time (TR) = 1300 msec, echo time (TE) = 42 msec, flip angle = 66°, bandwidth = 1924 Hz/pixel (0.64 msec echo spacing), posterior–anterior phase encoding, with fat saturation and "brain" shim mode. Distortion mapping scans, used to estimate the distortions present in the functional EPIs, were acquired with normal and reversed phase encoding after every other run. We used a 2-D SE-EPI with readout matching that of the GE-EPI and same number of slices, no slice acceleration, TE/TR = 45.6/3537 msec, three volumes. We used T1-weighted MPRAGE scans (0.8 × 0.8 × 0.8 mm voxels, field of view = 256 × 240 mm, TE/TR = 2.24/2400 msec, 192 slices, bandwidth = 210 Hz/pixel, turbo factor = 240, flip angle = 8°, inversion nonselective [inversion time = 1060 msec]) for gray matter segmentation, cortical flattening, registration, and visualization for creating ROIs.

fMRI Processing

Preprocessing

During preprocessing of functional data, we aligned the brain across runs and accounted for run- and session-specific distortions, with the aim of minimizing spatial transformations. This allowed us to maximize signal-to-noise ratio and minimize smoothing, ensuring data remain as near as possible to its original resolution. All preprocessing was done in Analysis of Functional NeuroImages (Version 17.3.09; (Cox, 1996). First, we corrected functional images for intensity inhomogeneity induced by the high-density receive coil by dividing all images by a smoothed bias field (15 mm FWHM), computed as the ratio of signal in the receive field image acquired using the head coil to that acquired using the in-bore "body" coil. Next, we estimated distortion and motion correction parameters. To minimize the effect of movement on the distortion correction (the distortion field depends on the exact position of the head in the main field), we collected multiple distortion correction scans throughout the experiment. Thus, every two functional runs flanked the distortion scans used to estimate these parameters. We refer to the functional–distortion–functional scan as a minisession. For each minisession, we used the distortion–correction procedure implemented in *afni_proc.py* to estimate parameters necessary to undistort and motion-correct functional images. Then, we used the estimated distortion field, motion correction transform for each volume, and functional-to-anatomical coregistration simultaneously to render functional data from native acquisition space into unwarped, motion-corrected, and coregistered anatomical space for

each participant at the same voxel size as data acquisition in a single transformation and resampling step. For each voxel on each run, we linearly detrended activation. We then computed percent signal change for each run.

Estimating Event-Related BOLD Activity

For each participant, we conducted a voxel-wise GLM to estimate each voxel's response to different trial events: precue, stimulus, delay, and response. The BOLD activity of a single voxel was predicted from a convolution of a canonical model of the hemodynamic impulse response function and a box-car regressor, which had length equal to each trial event.

Our main analysis investigated the effect of priority on the delay period. For all stimulus events that were not the delay period (precue, stimulus, and response epochs), we used one predictor each to estimate their activity across trials. For the delay period, we defined a predictor for each trial, so that we could have single-trial estimates of delay period activity. The GLM additionally contained predictors to account for motion and intercept for each run and were conducted in AFNI using *3dDeconvolve*.

Retinotopic Mapping

We used a recently developed pRF mapping approach (Mackey et al., 2017), which combines other pRF mapping approaches (Dumoulin & Wandell, 2008) with a more attentionally demanding task to map topographic areas in occipital, parietal, and frontal cortex. The methods are briefly summarized below; a more detailed description can be found in Mackey et al. (2017). During scanning, participants completed a difficult, covert attention task to ensure that required attention to the full spatial extent of the presented visual stimuli. The pRF mapping stimulus consisted of a bar subdivided into three random dot kinematograms (Williams & Sekuler, 1984; Figure 2A). The participant indicated with a button press which of the two flanker rectangles contained dots moving in the same mean direction as the center rectangle. The bar (horizontal or vertical orientation) swept across the entire visual field throughout the experiment, so that participants had to attend to the areas of the visual field that contained visual stimuli. Each sweep lasted 31.2 sec, and the bar updated its position every two TRs (2.6 sec). Each run consisted of 12 sweeps, and participants completed between 9 and 12 identical runs, which were averaged together before model fitting. Across sweeps, the width of the bar was varied among three discrete levels (1, 2, or 3 dva) to enable estimation of a nonlinear spatial summation model (Mackey et al., 2017; Kay, Winawer, Mezer, & Wandell, 2013).

We modeled the predicted response amplitude for each voxel at time t, $\hat{r}(t)$ using the following equation

$$\hat{r}(t) = \gamma \left[\int \int S(x,y) N((x,y), \mathbf{I}\sigma) \mathrm{d}x \mathrm{d}y \right]^n$$
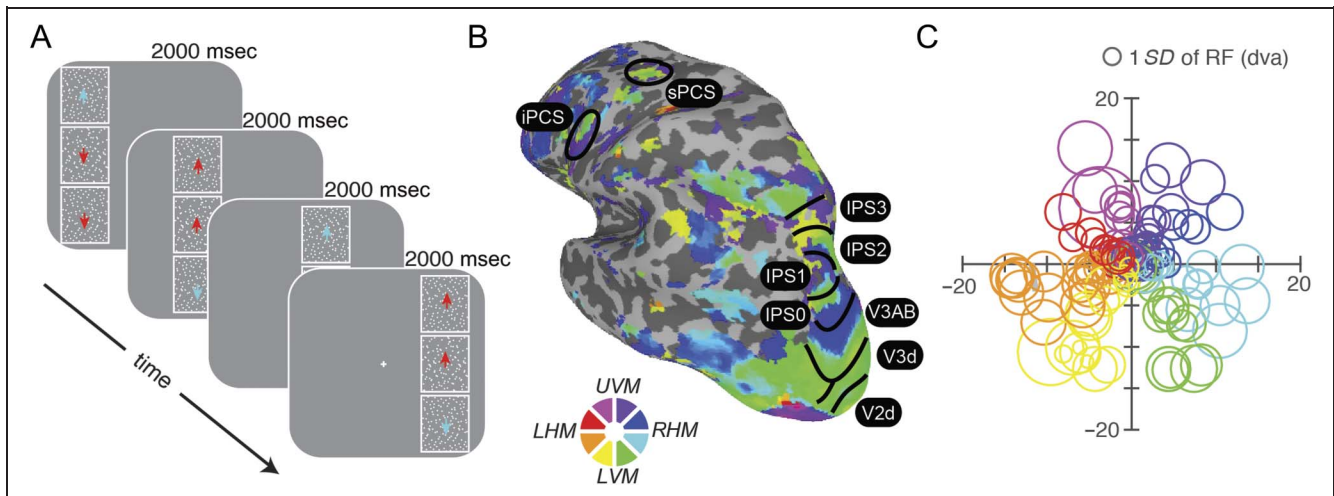
Figure 2. Measuring spatial selectivity of individual fMRI voxels via pRF mapping. (A) Behavioral task used for pRF mapping. Participants indicated with a button press which of the two flanker rectangles contained dots moving in the same mean direction as the center rectangle. The rectangle configuration could sweep horizontally (as illustrated) or vertically. The dots within each rectangle moved orthogonal to the direction of the rectangle movement. Data from this task were used to fit pRF models to each voxel (nonlinear compressive spatial summation; Mackey et al., 2017; Kay et al., 2013). (B) Example visual field maps plotted on an inflated surface view of the left cortex. The colors indicate the estimated polar angle center of each voxel's pRF, which are used to define ROIs. UVM/LVM = upper/lower vertical meridian; LHM/RHM = left/right horizontal meridian. Colored voxels indicate pRF model fit explains ≥10% variance. (C) Center position and standard deviation of 150 pRFs plotted from example participant's V3. Like receptive fields of individual neurons, the receptive fields of voxels have less concentration and larger receptive fields with increasing retinal eccentricity.

in which S is a binary stimulus image (1 sec where the stimulus was presented and 0 sec otherwise) and $N((x, y), \mathbf{I}\sigma)$ is a normal distribution with mean (x, y) and variance $\mathbf{I}\sigma^2$, where $\mathbf{I}$ is a two-dimensional identity matrix describing a circular, symmetric Gaussian. The parameters of this model are receptive field center (x, y), standard deviation σ, amplitude γ, and compressive spatial summation factor n (where $n \leq 1$). Parameters were fit with a GPU-accelerated course grid search over parameters, followed by a local optimization method.

We used the estimated parameters acquired from the pRF mapping to define visual field maps. Specifically, we used the estimates of the polar angle and eccentricity of each voxel as measured through the pRF model. We visualized flattened cortical surface representations (computed using Freesurfer 6.0) of each participant's brain using AFNI and SUMA (smoothed on the surface with a 5-mm kernel) and defined retinotopic maps based on standard conventions (Mackey et al., 2017; Wandell, Dumoulin, & Brewer, 2007; Larsson & Heeger, 2006). We defined the following areas: V1, V2, V3, V3AB, IPS0, IPS1, IP2, IPS3, iPCS, and sPCS (subset of left hemisphere regions visible in Figure 2B). In all further analyses, we use unsmoothed maps. First, we restricted our maps based on pRF estimates; we excluded voxels that did not have over 10% variance explained from the pRF model and voxels with RF centers nearer than 4 dva or farther than 20 dva eccentricity from fixation. We used a liberal exclusion criterion under the assumption that our analysis would essentially ignore voxels sensitive to locations far away from memorized item locations. Figure 2B illustrates the angle maps from an example participant, which demonstrates the topographic organization of visual field maps in occipital, parietal, and frontal cortical regions (Mackey et al., 2017).

Analyses

We used three types of analyses to address our primary research questions. First, we analyzed whether average activation in each area exhibited sustained elevated delay period activity. Second, we tested whether the delay period activation associated with individual items differed based on their cued priority. Although the first analysis asked whether the BOLD activity of an entire visual field map is elevated during the delay period, the second asked whether priority influences the "relative" profile of delay period activity within the map on each trial. Third, we tested if, across participants, those with a greater effect of priority on behavioral recall error also exhibited a greater effect of priority on item-specific delay period activity.

Univariate sustained activation analysis. First, we tested whether each visual field map exhibited elevated delay period activity. For each participant in each visual field map, we averaged all the delay period predictors, which we denote β, across trials and voxels to get one estimate of delay period activity. For each ROI, we evaluated statistical significance using parametric t tests (average β across participants compared against 0, one-tailed) as well as nonparametrically through bootstrapped confidence intervals (resampling the 11 participants' average betas, with replacement, a thousand times and comparing the proportion of resampled means below 0).

Item-specific delay period activation. Second, we tested whether the delay period activity varied based on cued priority associated with each individual item. The

goal of this analysis was to test whether the delay period activity was different for populations maintaining items at different priority levels. Although the previous analysis investigated if an entire visual field map had sustained activity through a delay period, this analysis tested whether the relative activity within a visual field map differed across different levels of priority.

To dissociate the delay period activity evoked by different items, we estimated item-specific population activities by adjusting the contribution of each voxel's delay period activity (estimated through GLM) according to its selectivity for each item's location. This means that the larger the overlap between a voxel's pRF and an item's location, the larger the contribution of that voxel in the overall activity evoked by that item. For every item in every trial, we computed a pRF-weighted β,

$$\beta_{pRF} = \frac{1}{N}\sum_{i}^{N} w_i(x)\beta_i$$

where $w_i(x)$ is the weight associated with the ith voxel at location x and β_i is the GLM-acquired delay period β at voxel i. We define w_i as the receptive field of voxel i, which we model in accordance with the pRF models; voxel i's receptive field is represented as a nonnormalized Gaussian with mean μ_i and variance σ_i^2,

$$w_i(x) = \exp\left(-\frac{(x - \mu_i)^2}{2\sigma_i^2}\right)$$

Thus, voxels have a higher weight when they are more tuned to an item's location. For example, when an item is at the voxel's receptive field center, or when $x = \mu_i$, the weight is $w_i(x) = 1$. As the Euclidean distance between x and μ_i increases, this weight decreases; the steepness with which it decreases is related to σ_i. This weighting is mathematically similar to pRF-weighted "stimulus reconstructions" reported previously (Kok & de Lange, 2014; Thirion et al., 2006) but evaluated at single points of the image (the item positions).

For each visual field map, we tested the effect of priority. First, for each participant, we conducted a linear regression with β_{pRF} as the dependent variable and priority level as the predictor. Then, we conducted a t test across participants to see if the priority predictor was above 0.

Effect of RF size on item-specific delay period activation. As a control analysis, we considered the possibility that systematic RF changes across ROIs could affect the results of our item-specific delay period activation analysis. For example, voxels in higher-level areas have larger RFs (Mackey et al., 2017; Kay et al., 2013; Dumoulin & Wandell, 2008), which could potentially result in more similar sensitivities (and thus pRF weights) across items. To test this hypothesis, we systematically changed the response field sizes of each voxel in each area. We then recalculated the β_{pRF}s for each priority and recalculated the slope. We investigated whether increasing the response field sizes decreased the slope of the priority effect and whether
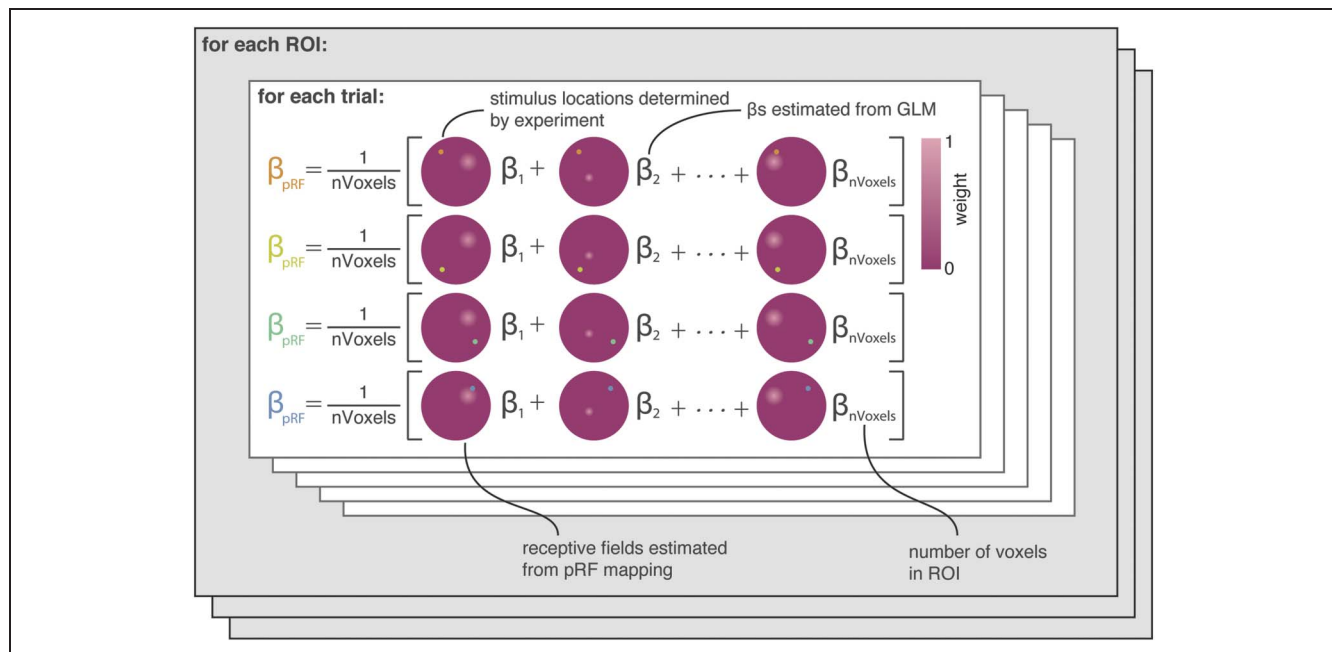

Figure 3. Procedure for estimating WM representation gain (β_{pRF}) based on pRF parameters. For each trial, we weight the GLM-obtained estimate of delay period activity for voxel i, β_i, by its sensitivity to the location of the current item as estimated by the pRF model. The heat plots illustrate the estimated receptive field over the entire stimulus display (a nonnormalized Gaussian distribution with a mode equivalent to weight = 1) for each voxel. The corresponding weight for each voxel is the scalar value at the item's location (the value at the colored dot). Each row here illustrates how the weights are updated across items within the same trial by changing the item's location (the colored dots on the receptive field maps). Across trials, the βs and stimulus locations are updated. Across ROIs, the voxels and their receptive fields are updated.

decreasing the response field sizes increased the slope of the priority effect.

Correlation between behavioral and neural data. Finally, we tested if, across participants, those with a greater effect of priority on behavioral recall error also exhibited a greater effect of priority on item-specific delay period activity. First, for each participant, we conducted two regressions to obtain an estimate of the effect of priority on behavioral and neural data separately. Then, we calculated the Pearson correlation across participants between the two slopes (one-tailed, based on the a priori prediction that increased delay period activation would be associated with decreased behavioral recall error).

RESULTS

Behavioral Results

To test our prediction that higher priority items would be remembered more precisely, we calculated memory error as a function of priority. We operationalized error as the Euclidean distance between the target location and the final saccade landing point. We conducted a linear regression testing whether error varied based on priority. We found that increasing priority significantly predicted a decrease in error ($b = -1.16$, $R^2 = .18$, $F = 6.67$, $p = .01$). This result was not due to a speed–accuracy trade off, because RTs also marginally decreased with increasing priority ($b = -0.12$, $R^2 = .09$, $F = 3.25$, $p = .08$). These results indicate that people remember higher priority items more precisely, consistent with previous reports (Yoo et al., 2018; Emrich et al., 2017; Bays, 2014; Klyszejko et al., 2014).

Neuroimaging Results

We investigated the effect of priority and WM over 10 retinotopically defined brain regions across dorsal visual, parietal, and frontal cortex: V1, V2, V3, V3AB, IPS0, IPS1, IPS2, IPS3, iPCS, and sPCS. For each brain area, we asked whether there was elevated delay activity in the entire region and then whether there was an item-specific effect
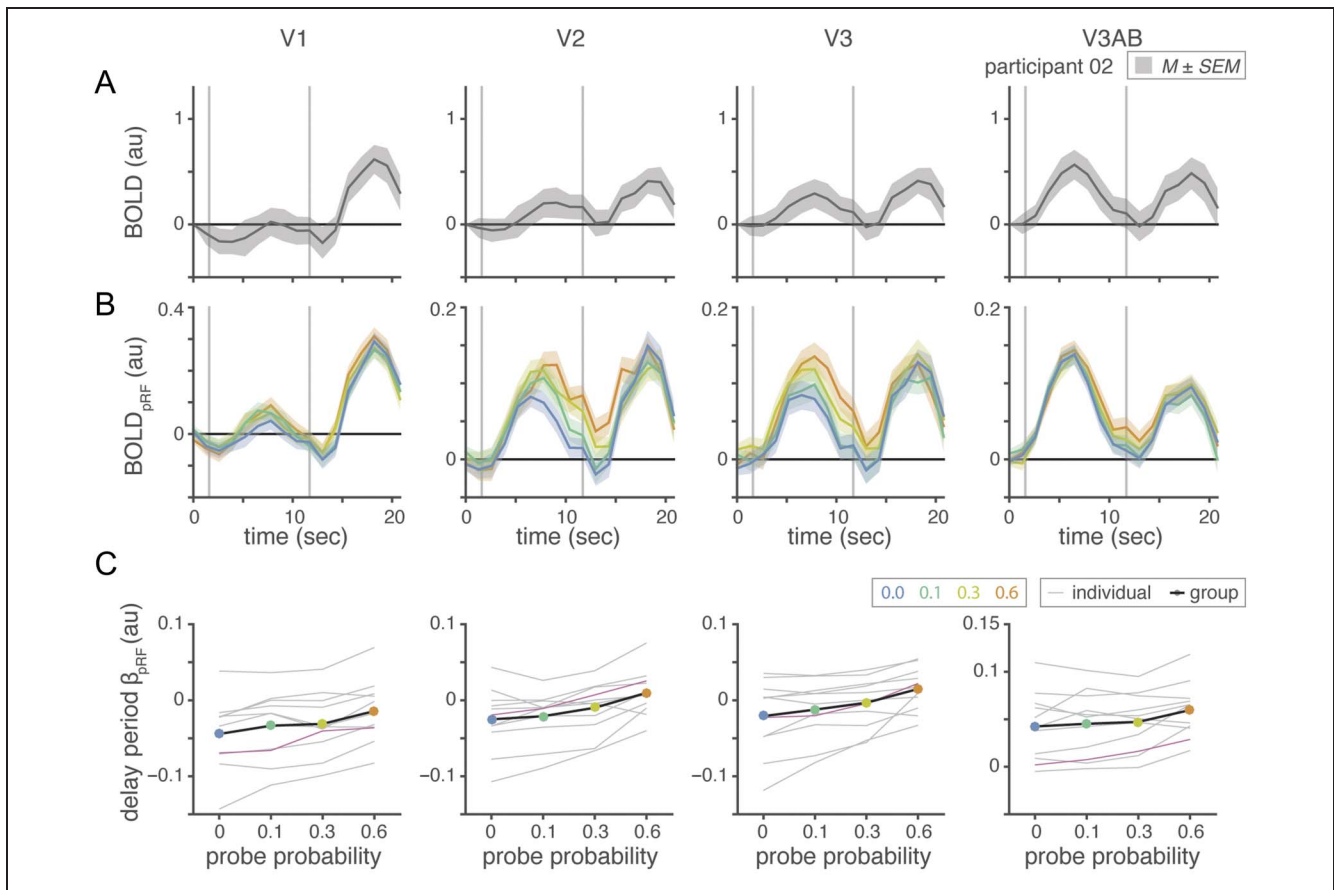

Figure 4. Priority modulates delay period activity in visual cortex. Univariate hemodynamic response function (HRF) time courses (A), β_{pRF}-weighted HRF time courses (B), and item-specific delay period activation (C) for visual areas V1, V2, V3, and V3AB (columns). (A) Average trial-related BOLD signal of an example participant ($M \pm SEM$ across trials), independent of priority showing event-related changes in BOLD activity. Univariate delay period activation does not have elevated delay period activity. (B) Average pRF-weighted BOLD signal of an example participant ($M \pm SEM$ across trials). Apparent separation of BOLD activity during time course corresponding to HRF of delay period. (C) β_{pRF} as a function of priority for individual participants (gray) and across participants (black), illustrating the priority modulation of β_{pRF}. Pink line indicates Participant 02, the example participant illustrated in panels A and B.

of priority on the magnitude of delay period activity within the region. For all statistics reported, p values were Bonferroni-corrected across ROIs.

Univariate Delay Period Activation

First, we tested whether any retinotopic regions showed elevated delay period activity when activation was averaged across voxels within the region. Delay period activity was quantified using a single-trial GLM approach (see Methods section). Early visual areas V1, V2, and V3 did not exhibit activity that was significantly higher than baseline (Figures 4A and 6A). However, dorsal visual region V3AB and all parietal and prefrontal regions tested did exhibit delay period activity that was significantly higher than baseline (Figures 5A and 6A; $p < .001$, for t test and bootstrapped significance test).

Item-specific Delay Period Activation

Second, we tested whether the delay period BOLD activity in voxels spatially selective for locations of different items differed based on the item's behavioral priority. We used each voxel's independently estimated pRF to quantify the

overall population activation associated with each item's spatial location on each trial (Figure 3; see Methods section). This resulted in measured activation levels corresponding to each WM item (.6, .3, .1, and .0 probe probability) on each trial (Figures 4B–C and 5B–C). We considered this analysis a higher-resolution investigation of the effect of the behavioral priority of multiple items on the measured priority map within an ROI. To establish whether the cued priority significantly sculpted activation strength in each ROIs retinotopic map, we first conducted a linear regression between the behavioral priority level and the item-specific delay period activity computed based on β_{pRF} for each participant (see Methods section). We then conducted a t test to investigate if the priority significantly predicted β_{pRF} with slope above 0.

Although there was no overall elevated delay period activation in visual areas (Figures 4A and 6A), the profile of activation within each region showed an effect of priority (Figures 4B–C and 6B). Priority was a significant modulator of delay period BOLD activity for V1, $t(10) = 6.47$, $p = .0007$; V2, $t(10) = 4.74$, $p = .007$; and V3, $t(10) = 4.13$, $p = .02$. Area V3AB was significant before Bonferroni correction, but trending afterward, $t(10) = 3.45$, $p = .06$. These results suggest that subpopulations in visual areas
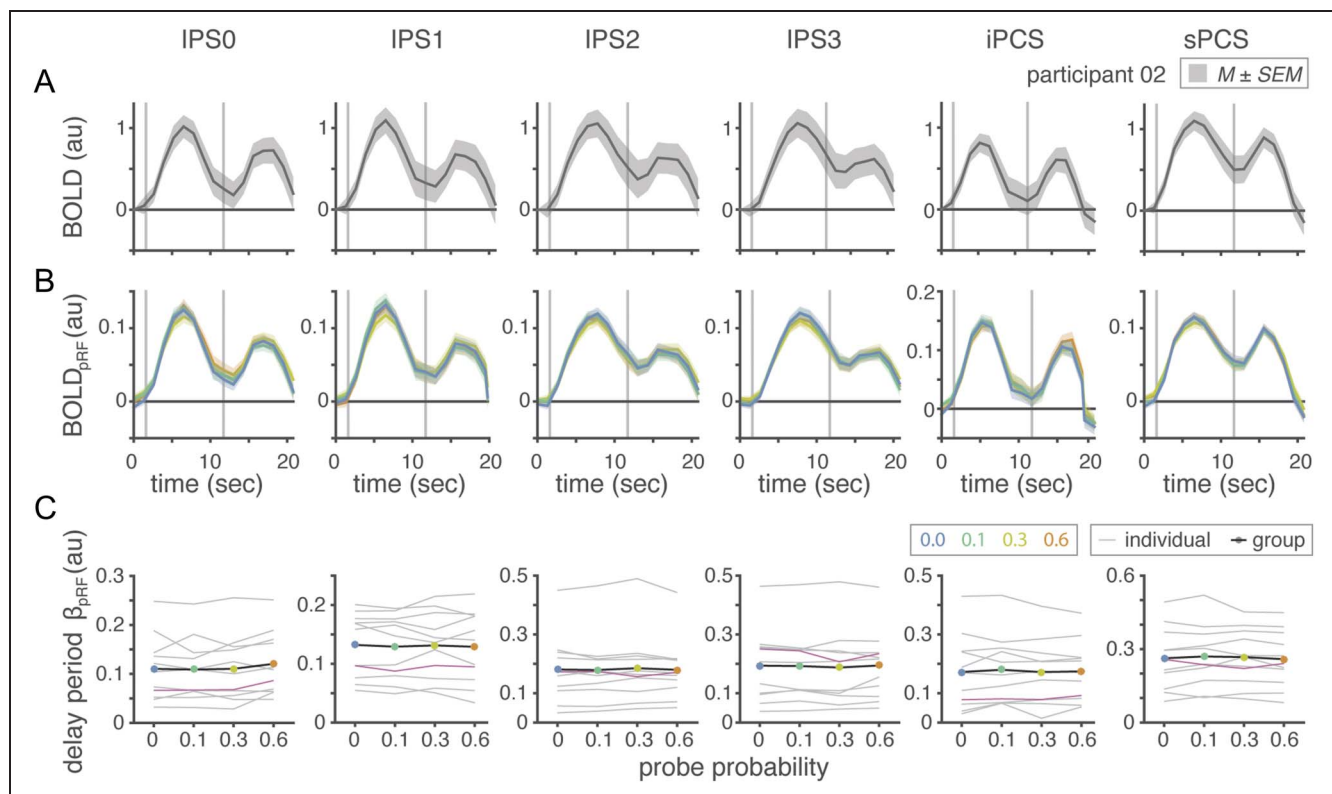

Figure 5. No effect of priority in delay activity in parietal and frontal areas. Univariate hemodynamic response function (HRF) time courses (A), β_{pRF}-weighted HRF time courses (B), and item-specific delay period activation (C) for parietal and frontal areas IPS0, IPS1, IPS2, IPS3, iPCS, and sPCS (columns). (A) Average trial-related BOLD signal of an example participant ($M \pm SEM$ across trials), independent of priority showing event-related changes in BOLD activity. Delay period shows an elevated delay period activity. (B) Average pRF-weighted BOLD signal of an example participant ($M \pm SEM$ across trials). No apparent separation of BOLD activity during time course corresponding to HRF of delay period. (C) β_{pRF} as a function of priority for individual participants (gray) and across participants (black). Pink line indicates Participant 02, the example participant illustrated in in panels A and B. There is no effect of priority on β_{pRF}.
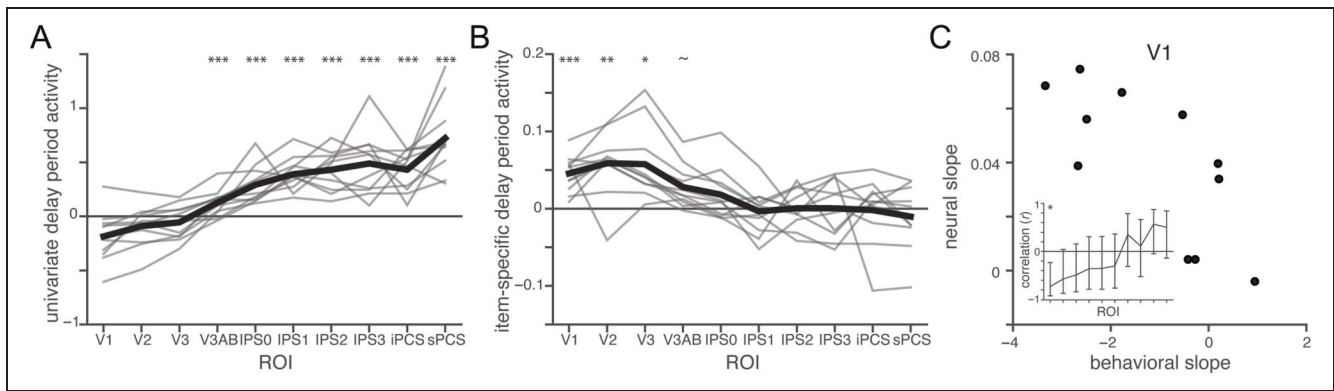
Figure 6. Summary of fMRI results. (A) Univariate delay period activity for each ROI, for individual participants (gray lines) and averaged across participants (black line) as estimated from GLM. Asterisks indicate ROIs that have delay period activity significantly higher than baseline after Bonferroni correction (***$p \le .001$). (B) Estimated slope of pRF-weighted delay period activity for individual participants (gray lines) and averaged across participants (black line). Asterisks indicate ROIs that have a significant effect of behavioral priority on item-specific delay period activity after Bonferroni correction (***$p \le .001$, **$p \le .01$, *$p \le .05$, ~$p \le .10$). (C) Scatter plot of neural and behavioral effects of priority across participants (black dots: individual participants). In V1, participants with a greater effect of priority on behavioral memory errors (higher priority, lower relative error) also have a greater effect of priority on BOLD responses (higher priority, higher relative item-specific delay period activity). Inset: 95% CI of interparticipant correlation between neural and behavioral slopes, for each ROI. Only V1 has a significant correlation after Bonferroni correction (*$p \le .05$).

corresponding to an item's location have higher delay period activity when maintaining a higher priority item (Figure 4B). On the other hand, there was no effect of priority on item-specific delay period activity in any frontoparietal region (Figures 5B–C and 6B).

To answer whether the lack of priority effect on item-specific delay period activity in frontoparietal cortex is simply a result of their larger RFs (Mackey et al., 2017; Kay et al., 2013; Dumoulin & Wandell, 2008), we estimated the effect of RF size on item-specific delay period activation. We found no consistent evidence that increasing or decreasing RF sizes results in a respective decrease or increase in the slope of the priority effect in each area. This indicated that our lack of significant priority-modulated item-specific delay period activation in the frontoparietal cortex was not simply due to large RFs (data not shown).

Correlation between Behavioral and Neural Data

Finally, we estimated correlations between neural and behavioral indices impacted by priority across participants. In V1, the priority of the items mediated a significant correlation between the amplitudes of item-specific delay period activity and the magnitudes of behavioral memory errors ($p = .05$, Bonferroni corrected). Specifically, participants whose delay period activation was more modulated by the priority of the items also produced memory errors more modulated by the priority of the items. Although we only found this effect to be significant in V1, the magnitude of these correlations decreased moving up along the visual hierarchy (Figure 6C), qualitatively corroborating our other findings.

DISCUSSION

In this study, we asked how the behavioral relevance of an item in WM modulates neural representations across the

brain. We hypothesized that an item's priority would be reflected in the amplitude of the same neural subpopulations that encode its location. To test this hypothesis, we collected fMRI BOLD activity while participants completed a multi-item spatial delayed estimation task and analyzed the delay period activity using traditional univariate metrics and a novel method informed by computational modeling of voxel receptive field properties. We found two main results: First, frontoparietal areas exhibited elevated delay period BOLD activity, on average, but did not exhibit priority-modulated item-specific activity; second, visual areas exhibited priority-modulated item-specific activity but little elevated delay period BOLD activity on average. The distinction between general delay period activity and prioritized item-specific activity suggests different roles across the processing hierarchy. What are these distinct roles, and how do they relate to WM theory?

Our results are consistent with decoding studies finding successful decoding of stimulus information from visual cortex despite a lack of sustained delay period activity (Ester, Sprague, & Serences, 2015; van Bergen, Ma, Pratte, & Jehee, 2015; Albers, Kok, Toni, Dijkerman, & de Lange, 2013; Lee, Kravitz, & Baker, 2013; Christophel et al., 2012; Riggall & Postle, 2012; Ester, Serences, & Awh, 2009; Harrison & Tong, 2009; Serences et al., 2009). Although the study was not designed to decode specific item positions, our observation that voxels with pRFs overlapping high-priority items exhibit greater delay period activation than voxels with pRFs overlapping lower-priority items suggests a mechanism whereby a prioritized item in memory is maintained with higher gain. Because our study made the very specific hypothesis that precision depends on the amplitude of the same neural subpopulations encoding an item's location during the WM delay, our results offer an explanation beyond previous decoding studies by explaining how behavioral priority may impact

neural codes, not merely determining whether it has an effect. Additionally, our results demonstrate that the attentional gain modulation during visual perception associated with a probabilistic precue (Sprague et al., 2018; Buracas & Boynton, 2007; Kastner et al., 1999; Somers et al., 1999) sustains throughout a WM delay.

Although we found differences in activation associated with remembered positions across priority levels in visual cortex, we did not find such an effect in frontal or parietal areas. We consider a variety of reasons for this surprising result. First, voxels have larger receptive fields in higher-level areas (Mackey et al., 2017; Kay et al., 2013; Dumoulin & Wandell, 2008), and this could cause pooling of responses (β_{pRF}s) across priorities. Although theoretical evidence suggests that populations with large RF sizes can precisely represent the locations of stimuli (Lehky & Sereno, 2011), we wondered if RF sizes could affect the results of our specific pRF-weighting analysis. However, a control analysis in which we simulated the impact of smaller and larger RF sizes indicated that differences in RF size alone could not account for our lack of item-specific priority results in frontoparietal areas. Second, we investigated the specific hypothesis that priority is coded by the amplitude of the same neural population encoding its location. Perhaps there are other ways priority may be neurally implemented. For example, priority could be represented through the variance in gain, rather than magnitude (Hénaff, Boundy-Singer, Meding, Ziemba, & Goris, 2020). Alternatively, priority could be supported by areas outside the populations maintaining the memorized locations. Finally, we assumed in our analyses that pRF estimates are stable across task conditions and thus are independent of stimulus and priority configuration. However, some evidence suggests that attention or set size manipulations, which may impact priority, can alter pRF parameters (Vo, Sprague, & Serences, 2017; Kay, Weiner, & Grill-Spector, 2015; Sheremata & Silver, 2015; Klein, Harvey, & Dumoulin, 2014; Sprague & Serences, 2013), and the effects of attention could differentially impact specific brain areas or even hemispheres (Sheremata & Silver, 2015; Klein et al., 2014). Although we acknowledge that our results depend on the assumption of stability, violations would only lead to poorer estimates of item-specific delay period activity. As we randomly assigned the locations and priorities of targets, any trial-specific fluctuations in pRFs should average out across trials. Thus, we do not believe our results in visual areas could be a result of these limitations.

A promising explanation for the role of sensory areas in WM comes from the sensory recruitment hypothesis, which posits that the same areas that process sensory information are also involved in the maintenance of sensory WM representation (Curtis & Sprague, 2021; Serences, 2016; Postle, 2006; Pasternak & Greenlee, 2005; Curtis & D'Esposito, 2003). One appealing aspect of this hypothesis relates to efficiency in that WM representations are precisely maintained in the same regions using the same mechanisms used for encoding percepts. Our results also appeal to efficiency as they demonstrate that the early visual areas that have been repeatedly shown to encode WM features also encode the relative priority of multiple WM items. Previous studies tested how changing an item's priority status over the course of a trial impacts the quality of decoded neural representations from visual, parietal, and frontal cortex (Iamshchinina, Christophel, & Gayet, 2021; Lorenc, Vandenbroucke, Nee, de Lange, & D'Esposito, 2020; Sahan, Sheldon, & Postle, 2020; Yu, Teng, & Postle, 2020; Christophel, Iamshchinina, Yan, Allefeld, & Haynes, 2018; Rahmati et al., 2018; LaRocque, Riggall, Emrich, & Postle, 2017; Rose et al., 2016; Sprague et al., 2016; Lewis-Peacock, Drysdale, Oberauer, & Postle, 2012). In many of these studies, experimenters employed a "dual retrocue" task, in which cues presented during the delay period allow participants to transiently prioritize one of multiple items for an upcoming response. Importantly, when an item is cued, the cue is often 100% valid, and so any noncued items can be transiently deprioritized. Consequently, these tasks do not test how multiple items of continuously varying priority states are represented simultaneously. However, they have the unique ability to compare coding properties of WM representations imminently relevant for behavior to those relevant at a later time point. Results from these studies vary and suggest that only immediately relevant WM representations can be decoded (Lorenc et al., 2020; Sahan et al., 2020; Yu et al., 2020), that both prioritized and nonprioritized WM representations can be decoded with sufficient sample size (Christophel et al., 2018), or that results critically depend on particulars of the multivariate analysis procedures employed (Iamshchinina et al., 2021). Using an antisaccade procedure, where the goal of a memory-guided saccade was opposite the visual target, we recently demonstrated that the strength of WM representations in early visual cortex migrated from the visual target early in the delay to the saccade goal later in the delay (Rahmati et al., 2018). In light of the current results, we argue that the priority of the two locations changed during the course of the trial as the location of the visual stimulus was recoded into the location of the memory-guided saccade. Indeed, future studies employing dynamic reprioritization of spatial positions throughout a trial (e.g., Sprague et al., 2016) may help triangulate how graded relative priority and transient reliable priority compare to one another.

The relationship between behavioral priority and neural gain is consistent with probabilistic population coding models of WM, which predict that increased neural gain increases signal-to-noise ratio in neural populations, resulting in higher behavioral precision (Bays, 2014). Probabilistic population coding models posit that neural populations themselves represent a probability distribution over a stimulus representation, such that increased neural response gain corresponds to more precise representations of that stimulus (Ma, Beck, Latham, & Pouget, 2006; Zemel, Dayan, & Pouget, 1998). In WM tasks,

population coding models have used neural gain as a proxy for the memory precision of items and are able to account for the effects of prioritization on memory error (Bays, 2014; Ma et al., 2006; Seung & Sompolinsky, 1993). Here, we extend these previous results by showing that the relative priority assigned to each of several remembered positions modulates delay period activation in a graded fashion and that these activation profiles are associated with behavioral recall performance. These results are also consistent with our recent studies demonstrating that decoding errors in visual cortex predict memory errors (Hallenbeck et al., 2021; Li, Sprague, Yoo, Ma, & Curtis, 2021). In the current study, we demonstrated how priority moderates these neural and behavioral correlations. Across participants, the degree to which priority sculpted the gain of delay period activity in V1 predicted the degree to which priority impacted the quality of WM representations. Such a priority-mediated coupling suggests a potential mechanism for the large individual differences observed across people in WM abilities (Luck & Vogel, 2013).

Our results in frontoparietal areas are especially interesting in reference to decoding studies that typically find an absence of stimulus information in frontoparietal regions despite elevated delay period activity (e.g., Emrich, Riggall, Larocque, & Postle, 2013; Christophel et al., 2012; Riggall & Postle, 2012; Postle, Druzgal, & D'Esposito, 2003; but see Hallenbeck et al., 2021; Ester et al., 2015; Jerde et al., 2012). Because our study tested the very specific hypothesis that precision is mediated by the gain of the neural subpopulations encoding an item's location in memory, these results cannot be used as evidence that all representations of priority are absent in the frontal or parietal cortex. Rather than prioritizing specific items, perhaps frontal cortex prioritizes more general behaviors such as the broader goals of the task (i.e., utilize the priority cues and remember the locations of the items). Indeed, one can decode from frontal cortex task-relevant information (i.e., stimulus dimension) but not stimulus information (i.e., specific stimulus feature; Riggall & Postle, 2012; but see Ester et al., 2015). Thus, pFC may encode task demands more than low-level physical properties of stimuli (Christophel, Cichy, Hebart, & Haynes, 2015; Christophel & Haynes, 2014; McKee, Riesenhuber, Miller, & Freedman, 2014; Emrich et al., 2013; Christophel et al., 2012; Riggall & Postle, 2012; Warden & Miller, 2010; Wallis & Miller, 2003; Freedman, Riesenhuber, Poggio, & Miller, 2001, 2002; Wallis, Anderson, & Miller, 2001; White & Wise, 1999).

In summary, our study adds to the growing body of literature connecting activation patterns in visual areas to high-fidelity WM representations in the brain. By applying a novel pRF-guided analysis method, we demonstrated that voxels tuned to higher-priority locations held in WM exhibited greater BOLD activation during the delay period, consistent with a higher-precision representation, which we observed behaviorally. Modulating neural gain may be a key mechanism whereby neural systems dynamically optimize processing resources to support cognitive demands.

Data and Code Availability

Processed, deidentified data is available through the Open Science Framework (https://osf.io/jsuw6/). The raw fMRI data are available under restricted access to ensure participant privacy; access can be obtained by contacting the corresponding author. Analysis and plotting code publicly available at https://github.com/aspenyoo/priority _precision_gain.

Auhor Contributions

Aspen H. Yoo: Formal analysis; Methodology; Software; Visualization; Writing—Original draft; Writing—Review & editing. Alfredo Bolaños: Data curation; Formal analysis. Grace E. Hallenbeck: Data curation; Formal analysis; Software; Supervision; Visualization; Writing—Review & editing. Masih Rahmati: Formal analysis; Methodology; Writing—Review & editing. Thomas C. Sprague: Methodology; Software; Supervision; Visualization; Writing—Review & editing. Clayton E. Curtis: Conceptualization; Data curation; Funding acquisition; Investigation; Methodology; Project administration; Supervision; Visualization; Writing—Original draft; Writing—Review & editing.

Diversity in Citation Practices

A retrospective analysis of the citations in every article published in this journal from 2010 to 2020 has revealed a persistent pattern of gender imbalance: Although the proportions of authorship teams (categorized by estimated gender identification of first author/last author) publishing in the *Journal of Cognitive Neuroscience* (*JoCN*) during

this period were M(an)/M = .408, W(oman)/M = .335, M/W = .108, and W/W = .149, the comparable proportions for the articles that these authorship teams cited were M/M = .579, W/M = .243, M/W = .102, and W/W = .076 (Fulvio et al., *JoCN*, 33:1, pp. 3–7). Consequently, *JoCN* encourages all authors to consider gender balance explicitly when selecting which articles to cite and gives them the opportunity to report their article's gender citation balance.

REFERENCES

Albers, A. M., Kok, P., Toni, I., Dijkerman, H. C., & de Lange, F. P. (2013). Shared representations for working memory and mental imagery in early visual cortex. *Current Biology*, *23*, 1427–1431. https://doi.org/10.1016/j.cub.2013.05.065, PubMed: 23871239

Bays, P. M. (2014). Noise in neural populations accounts for errors in working memory. *Journal of Neuroscience*, *34*, 3632–3645. https://doi.org/10.1523/JNEUROSCI.3204-13.2014, PubMed: 24599462

Bisley, J. W., & Goldberg, M. E. (2010). Attention, intention, and priority in the parietal lobe. *Annual Review of Neuroscience*, *33*, 1–21. https://doi.org/10.1146/annurev-neuro-060909-152823, PubMed: 20192813

Brainard, D. H. (1997). The psychophysics toolbox. *Spatial Vision*, *10*, 433–436. https://doi.org/10.1163/156856897x00357, PubMed: 9176952

Buracas, G. T., & Boynton, G. M. (2007). The effect of spatial attention on contrast response functions in human visual cortex. *Journal of Neuroscience*, *27*, 93–97. https://doi.org/10.1523/jneurosci.3162-06.2007, PubMed: 17202476

Christophel, T. B., Cichy, R. M., Hebart, M. N., & Haynes, J.-D. (2015). Parietal and early visual cortices encode working memory content across mental transformations. *Neuroimage*, *106*, 198–206. https://doi.org/10.1016/j.neuroimage.2014.11.018, PubMed: 25463456

Christophel, T. B., & Haynes, J.-D. (2014). Decoding complex flow-field patterns in visual working memory. *Neuroimage*, *91*, 43–51. https://doi.org/10.1016/j.neuroimage.2014.01.025, PubMed: 24480302

Christophel, T. B., Hebart, M. N., & Haynes, J.-D. (2012). Decoding the contents of visual short-term memory from human visual and parietal cortex. *Journal of Neuroscience*, *32*, 12983–12989. https://doi.org/10.1523/JNEUROSCI.0184-12.2012, PubMed: 22993415

Christophel, T. B., Iamshchinina, P., Yan, C., Allefeld, C., & Haynes, J.-D. (2018). Cortical specialization for attended versus unattended working memory. *Nature Neuroscience*, *21*, 494–496. https://doi.org/10.1038/s41593-018-0094-4, PubMed: 29507410

Christophel, T. B., Klink, P. C., Spitzer, B., Roelfsema, P. R., & Haynes, J.-D. (2017). The distributed nature of working memory. *Trends in Cognitive Sciences*, *21*, 111–124. https://doi.org/10.1016/j.tics.2016.12.007, PubMed: 28063661

Courtney, S. M., Petit, L., Maisog, J. M., Ungerleider, L. G., & Haxby, J. V. (1998). An area specialized for spatial working memory in human frontal cortex. *Science*, *279*, 1347–1351. https://doi.org/10.1126/science.279.5355.1347, PubMed: 9478894

Cox, R. W. (1996). AFNI: Software for analysis and visualization of functional magnetic resonance neuroimages. *Computers and Biomedical Research*, *29*, 162–173. https://doi.org/10.1006/cbmr.1996.0014, PubMed: 8812068

Curtis, C. E., & D'Esposito, M. (2003). Persistent activity in the prefrontal cortex during working memory. *Trends in Cognitive Sciences*, *7*, 415–423. https://doi.org/10.1016/S1364-6613(03)00197-9

Curtis, C. E., Rao, V. Y., & D'Esposito, M. (2004). Maintenance of spatial and motor codes during oculomotor delayed response tasks. *Journal of Neuroscience*, *24*, 3944–3952. https://doi.org/10.1523/JNEUROSCI.5640-03.2004, PubMed: 15102910

Curtis, C. E., & Sprague, T. C. (2021). Persistent activity during working memory from front to back. *Frontiers in Neural Circuits*, *15*, 696060. https://doi.org/10.3389/fncir.2021.696060, PubMed: 34366794

Daneman, M., & Carpenter, P. A. (1980). Individual differences in working memory and reading. *Journal of Verbal Learning and Verbal Behavior*, *19*, 450–466. https://doi.org/10.1016/S0022-5371(80)90312-6

Dumoulin, S. O., & Wandell, B. A. (2008). Population receptive field estimates in human visual cortex. *Neuroimage*, *39*, 647–660. https://doi.org/10.1016/j.neuroimage.2007.09.034, PubMed: 17977024

Emrich, S. M., Lockhart, H. A., & Al-Aidroos, N. (2017). Attention mediates the flexible allocation of visual working memory resources. *Journal of Experimental Psychology: Human Perception and Performance*, *43*, 1454–1465. https://doi.org/10.1037/xhp0000398, PubMed: 28368161

Emrich, S. M., Riggall, A. C., Larocque, J. J., & Postle, B. R. (2013). Distributed patterns of activity in sensory cortex reflect the precision of multiple items maintained in visual short-term memory. *Journal of Neuroscience*, *33*, 6516–6523. https://doi.org/10.1523/JNEUROSCI.5732-12.2013, PubMed: 23575849

Engle, R. W., Tuholski, S. W., Laughlin, J. E., & Conway, A. R. A. (1999). Working memory, short-term memory, and general fluid intelligence: A latent-variable approach. *Journal of Experimental Psychology: General*, *128*, 309–331. https://doi.org/10.1037/0096-3445.128.3.309, PubMed: 10513398

Ester, E. F., Serences, J. T., & Awh, E. (2009). Spatially global representations in human primary visual cortex during working memory maintenance. *Journal of Neuroscience*, *29*, 15258–15265. https://doi.org/10.1523/JNEUROSCI.4388-09.2009, PubMed: 19955378

Ester, E. F., Sprague, T. C., & Serences, J. T. (2015). Parietal and frontal cortex encode stimulus-specific mnemonic representations during visual working memory. *Neuron*, *87*, 893–905. https://doi.org/10.1016/j.neuron.2015.07.013, PubMed: 26257053

Fecteau, J. H., & Munoz, D. P. (2006). Salience, relevance, and firing: A priority map for target selection. *Trends in Cognitive Sciences*, *10*, 382–390. https://doi.org/10.1016/j.tics.2006.06.011, PubMed: 16843702

Feinberg, D. A., Moeller, S., Smith, S. M., Auerbach, E., Ramanna, S., Gunther, M., et al. (2010). Multiplexed echo planar imaging for sub-second whole brain fMRI and fast diffusion imaging. *PLoS One*, *5*, e15710. https://doi.org/10.1371/journal.pone.0015710, PubMed: 21187930

Freedman, D. J., Riesenhuber, M., Poggio, T., & Miller, E. K. (2001). Categorical representation of visual stimuli in the primate prefrontal cortex. *Science*, *291*, 312–316. https://doi.org/10.1126/science.291.5502.312, PubMed: 11209083

Freedman, D. J., Riesenhuber, M., Poggio, T., & Miller, E. K. (2002). Visual categorization and the primate prefrontal cortex: Neurophysiology and behavior. *Journal of Neurophysiology*, *88*, 929–941. https://doi.org/10.1152/jn.2002.88.2.929, PubMed: 12163542

Funahashi, S., Bruce, C. J., & Goldman-Rakic, P. S. (1989). Mnemonic coding of visual space in the monkey's dorsolateral prefrontal cortex. *Journal of Neurophysiology*,

61, 331–349. https://doi.org/10.1152/jn.1989.61.2.331, PubMed: 2918358

Fuster, J. M., & Alexander, G. E. (1971). Neuron activity related to short-term memory. *Science*, *173*, 652–654. https://doi.org/10.1126/science.173.3997.652

Gandhi, S. P., Heeger, D. J., & Boynton, G. M. (1999). Spatial attention affects brain activity in human primary visual cortex. *Proceedings of the National Academy of Sciences, U.S.A.*, *96*, 3314–3319. https://doi.org/10.1073/pnas.96.6.3314, PubMed: 10077681

Gouws, A. D., Alvarez, I., Watson, D., Uesaki, M., Rodgers, J., & Morland, A. B. (2014). The role of cortical and subcortical suppression in spatial attention. *Journal of Vision*, *14*, 618–618. https://doi.org/10.1167/14.10.618

Hallenbeck, G. E., Sprague, T. C., Rahmati, M., Sreenivasan, K. K., & Curtis, C. E. (2021). Working memory representations in visual cortex mediate distraction effects. *Nature Communications*, *12*, 4714. https://doi.org/10.1038/s41467-021-24973-1, PubMed: 34354071

Harrison, S. A., & Tong, F. (2009). Decoding reveals the contents of visual working memory in early visual areas. *Nature*, *458*, 632–635. https://doi.org/10.1038/nature07832, PubMed: 19225460

Hénaff, O. J., Boundy-Singer, Z. M., Meding, K., Ziemba, C. M., & Goris, R. L. T. (2020). Representation of visual uncertainty through neural gain variability. *Nature Communications*, *11*, 2513. https://doi.org/10.1038/s41467-020-15533-0, PubMed: 32427825

Iamshchinina, P., Christophel, T. B., & Gayet, S. (2021). Essential considerations for exploring visual working memory storage in the human brain. *Visual Cognition*, *29*, 425–436. https://doi.org/10.1080/13506285.2021.1915902

Jerde, T. A., Merriam, E. P., Riggall, A. C., Hedges, J. H., & Curtis, C. E. (2012). Prioritized maps of space in human frontoparietal cortex. *Journal of Neuroscience*, *32*, 17382–17390. https://doi.org/10.1523/JNEUROSCI.3810-12.2012, PubMed: 23197729

Kastner, S., Pinsk, M. A., De Weerd, P., Desimone, R., & Ungerleider, L. G. (1999). Increased activity in human visual cortex during directed attention in the absence of visual stimulation. *Neuron*, *22*, 751–761. https://doi.org/10.1016/S0896-6273(00)80734-5, PubMed: 10230795

Kay, K. N., Weiner, K. S., & Grill-Spector, K. (2015). Attention reduces spatial uncertainty in human ventral temporal cortex. *Current Biology*, *25*, 595–600. https://doi.org/10.1016/j.cub.2014.12.050, PubMed: 25702580

Kay, K. N., Winawer, J., Mezer, A., & Wandell, B. A. (2013). Compressive spatial summation in human visual cortex. *Journal of Neurophysiology*, *110*, 481–494. https://doi.org/10.1152/jn.00105.2013, PubMed: 23615546

Klein, B. P., Harvey, B. M., & Dumoulin, S. O. (2014). Attraction of position preference by spatial attention throughout human visual cortex. *Neuron*, *84*, 227–237. https://doi.org/10.1016/j.neuron.2014.08.047, PubMed: 25242220

Klyszejko, Z., Rahmati, M., & Curtis, C. E. (2014). Attentional priority determines working memory precision. *Vision Research*, *105*, 70–76. https://doi.org/10.1016/j.visres.2014.09.002, PubMed: 25240420

Kok, P., & de Lange, F. P. (2014). Shape perception simultaneously up- and downregulates neural activity in the primary visual cortex. *Current Biology*, *24*, 1531–1535. https://doi.org/10.1016/j.cub.2014.05.042, PubMed: 24980501

LaRocque, J. J., Riggall, A. C., Emrich, S. M., & Postle, B. R. (2017). Within-category decoding of information in different attentional states in short-term memory. *Cerebral Cortex*, *27*, 4881–4890. https://doi.org/10.1093/cercor/bhw283, PubMed: 27702811

Larsson, J., & Heeger, D. J. (2006). Two retinotopic visual areas in human lateral occipital cortex. *Journal of Neuroscience*,

26, 13128–13142. https://doi.org/10.1523/JNEUROSCI.1657-06.2006, PubMed: 17182764

Lee, S.-H., Kravitz, D. J., & Baker, C. I. (2013). Goal-dependent dissociation of visual and prefrontal cortices during working memory. *Nature Neuroscience*, *16*, 997–999. https://doi.org/10.1038/nn.3452, PubMed: 23817547

Lehky, S. R., & Sereno, A. B. (2011). Population coding of visual space: Modeling. *Frontiers in Computational Neuroscience*, *4*, 155. https://doi.org/10.3389/fncom.2010.00155, PubMed: 21344012

Lewis-Peacock, J. A., Drysdale, A. T., Oberauer, K., & Postle, B. R. (2012). Neural evidence for a distinction between short-term memory and the focus of attention. *Journal of Cognitive Neuroscience*, *24*, 61–79. https://doi.org/10.1162/jocn_a_00140, PubMed: 21955164

Li, H.-H., Sprague, T. C., Yoo, A. H., Ma, W. J., & Curtis, C. E. (2021). Joint representation of working memory and uncertainty in human cortex. *Neuron*, *109*, 3699–3712. https://doi.org/10.1016/j.neuron.2021.08.022, PubMed: 34525327

Lorenc, E. S., Vandenbroucke, A. R. E., Nee, D. E., de Lange, F. P., & D'Esposito, M. (2020). Dissociable neural mechanisms underlie currently-relevant, future-relevant, and discarded working memory representations. *Scientific Reports*, *10*, 1–17. https://doi.org/10.1038/s41598-020-67634-x, PubMed: 32641712

Luck, S. J., & Vogel, E. K. (2013). Visual working memory capacity: From psychophysics and neurobiology to individual differences. *Trends in Cognitive Sciences*, *17*, 391–400. https://doi.org/10.1016/j.tics.2013.06.006, PubMed: 23850263

Ma, W. J., Beck, J. M., Latham, P. E., & Pouget, A. (2006). Bayesian inference with probabilistic population codes. *Nature Neuroscience*, *9*, 1432–1438. https://doi.org/10.1038/nn1790, PubMed: 17057707

Mackey, W. E., Winawer, J., & Curtis, C. E. (2017). Visual field map clusters in human frontoparietal cortex. *eLife*, *6*, e22974. https://doi.org/10.7554/eLife.22974, PubMed: 28628004

McCarthy, G., Blamire, A. M., Puce, A., Nobre, A. C., Bloch, G., Hyder, F., et al. (1994). Functional magnetic resonance imaging of human prefrontal cortex activation during a spatial working memory task. *Proceedings of the National Academy of Sciences, U.S.A.*, *91*, 8690–8694. https://doi.org/10.1073/pnas.91.18.8690, PubMed: 8078943

McKee, J. L., Riesenhuber, M., Miller, E. K., & Freedman, D. J. (2014). Task dependence of visual and category representations in prefrontal and inferior temporal cortices. *Journal of Neuroscience*, *34*, 16065–16075. https://doi.org/10.1523/JNEUROSCI.1660-14.2014, PubMed: 25429147

Moeller, S., Yacoub, E., Olman, C. A., Auerbach, E., Strupp, J., Harel, N., et al. (2010). Multiband multislice GE-EPI at 7 tesla, with 16-fold acceleration using partial parallel imaging with application to high spatial and temporal whole-brain fMRI. *Magnetic Resonance in Medicine*, *63*, 1144–1153. https://doi.org/10.1002/mrm.22361, PubMed: 20432285

Nobre, A. C., Coull, J. T., Maquet, P., Frith, C. D., Vandenberghe, R., & Mesulam, M. M. (2004). Orienting attention to locations in perceptual versus mental representations. *Journal of Cognitive Neuroscience*, *16*, 363–373. https://doi.org/10.1162/089892904322926700, PubMed: 15072672

Pasternak, T., & Greenlee, M. W. (2005). Working memory in primate sensory systems. *Nature Reviews Neuroscience*, *6*, 97–107. https://doi.org/10.1038/nrn1603, PubMed: 15654324

Pelli, D. G. (1997). The videotoolbox software for visual psychophysics: Transforming numbers into movies. *Spatial Vision*, *10*, 437–442. https://doi.org/10.1163/156856897x00366, PubMed: 9176953

Postle, B. R. (2006). Working memory as an emergent property of the mind and brain. *Neuroscience*, *139*, 23–38. https://doi.org/10.1016/j.neuroscience.2005.06.005, PubMed: 16324795

Postle, B. R., Druzgal, T. J., & D'Esposito, M. (2003). Seeking the neural substrates of visual working memory storage. *Cortex*, *39*, 927–946. https://doi.org/10.1016/S0010-9452(08)70871-2, PubMed: 14584560

Rahmati, M., Saber, G. T., & Curtis, C. E. (2018). Population dynamics of early visual cortex during working memory. *Journal of Cognitive Neuroscience*, *30*, 219–233. https://doi.org/10.1162/jocn_a_01196, PubMed: 28984524

Riggall, A. C., & Postle, B. R. (2012). The relationship between working memory storage and elevated activity as measured with functional magnetic resonance imaging. *Journal of Neuroscience*, *32*, 12990–12998. https://doi.org/10.1523/JNEUROSCI.1892-12.2012, PubMed: 22993416

Rose, N. S., LaRocque, J. J., Riggall, A. C., Gosseries, O., Starrett, M. J., Meyering, E. E., et al. (2016). Reactivation of latent working memories with transcranial magnetic stimulation. *Science*, *354*, 1136–1139. https://doi.org/10.1126/science.aah7011, PubMed: 27934762

Rowe, J. B., Toni, I., Josephs, O., Frackowiak, R. S., & Passingham, R. E. (2000). The prefrontal cortex: Response selection or maintenance within working memory? *Science*, *288*, 1656–1660. https://doi.org/10.1126/science.288.5471.1656, PubMed: 10834847

Saber, G. T., Pestilli, F., & Curtis, C. E. (2015). Saccade planning evokes topographically specific activity in the dorsal and ventral streams. *Journal of Neuroscience*, *35*, 245–252. https://doi.org/10.1523/JNEUROSCI.1687-14.2015, PubMed: 25568118

Sahan, M. I., Sheldon, A. D., & Postle, B. R. (2020). The neural consequences of attentional prioritization of internal representations in visual working memory. *Journal of Cognitive Neuroscience*, *32*, 917–944. https://doi.org/10.1162/jocn_a_01517, PubMed: 31851592

Schluppeck, D., Curtis, C. E., Glimcher, P. W., & Heeger, D. J. (2006). Sustained activity in topographic areas of human posterior parietal cortex during memory-guided saccades. *Journal of Neuroscience*, *26*, 5098–5108. https://doi.org/10.1523/JNEUROSCI.5330-05.2006, PubMed: 16687501

Serences, J. T. (2016). Neural mechanisms of information storage in visual short-term memory. *Vision Research*, *128*, 53–67. https://doi.org/10.1016/j.visres.2016.09.010, PubMed: 27668990

Serences, J. T., Ester, E. F., Vogel, E. K., & Awh, E. (2009). Stimulus-specific delay activity in human primary visual cortex. *Psychological Science*, *20*, 207–214. https://doi.org/10.1111/j.1467-9280.2009.02276.x, PubMed: 19170936

Serences, J. T., & Yantis, S. (2006). Selective visual attention and perceptual coherence. *Trends in Cognitive Sciences*, *10*, 38–45. https://doi.org/10.1016/j.tics.2005.11.008, PubMed: 16318922

Serences, J. T., & Yantis, S. (2007). Spatially selective representations of voluntary and stimulus-driven attentional priority in human occipital, parietal, and frontal cortex. *Cerebral Cortex*, *17*, 284–293. https://doi.org/10.1093/cercor/bhj146, PubMed: 16514108

Seung, H. S., & Sompolinsky, H. (1993). Simple models for reading neuronal population codes. *Proceedings of the National Academy of Sciences, U.S.A.*, *90*, 10749–10753. https://doi.org/10.1073/pnas.90.22.10749, PubMed: 8248166

Sheremata, S. L., & Silver, M. A. (2015). Hemisphere-dependent attentional modulation of human parietal visual field representations. *Journal of Neuroscience*, *35*, 508–517. https://doi.org/10.1523/JNEUROSCI.2378-14.2015, PubMed: 25589746

Somers, D. C., Dale, A. M., Seiffert, A. E., & Tootell, R. B. (1999). Functional MRI reveals spatially specific attentional modulation in human primary visual cortex. *Proceedings of the National Academy of Sciences, U.S.A.*, *96*, 1663–1668. https://doi.org/10.1073/pnas.96.4.1663, PubMed: 9990081

Sprague, T. C., Ester, E. F., & Serences, J. T. (2014). Reconstructions of information in visual spatial working memory degrade with memory load. *Current Biology*, *24*, 2174–2180. https://doi.org/10.1016/j.cub.2014.07.066, PubMed: 25201683

Sprague, T. C., Ester, E. F., & Serences, J. T. (2016). Restoring latent visual working memory representations in human cortex. *Neuron*, *91*, 694–707. https://doi.org/10.1016/j.neuron.2016.07.006, PubMed: 27497224

Sprague, T. C., Itthipuripat, S., Vo, V. A., & Serences, J. T. (2018). Dissociable signatures of visual salience and behavioral relevance across attentional priority maps in human cortex. *Journal of Neurophysiology*, *119*, 2153–2165. https://doi.org/10.1152/jn.00059.2018, PubMed: 29488841

Sprague, T. C., & Serences, J. T. (2013). Attention modulates spatial priority maps in the human occipital, parietal and frontal cortices. *Nature Neuroscience*, *16*, 1879–1887. https://doi.org/10.1038/nn.3574, PubMed: 24212672

Süß, H.-M., Oberauer, K., Wittmann, W. W., Wilhelm, O., & Schulze, R. (2002). Working-memory capacity explains reasoning ability—And a little bit more. *Intelligence*, *30*, 261–288. https://doi.org/10.1016/S0160-2896(01)00100-3

Thirion, B., Duchesnay, E., Hubbard, E., Dubois, J., Poline, J.-B., Lebihan, D., et al. (2006). Inverse retinotopy: Inferring the visual content of images from brain activation patterns. *Neuroimage*, *33*, 1104–1116. https://doi.org/10.1016/j.neuroimage.2006.06.062, PubMed: 17029988

Thompson, K. G., & Bichot, N. P. (2005). A visual salience map in the primate frontal eye field. *Progress in Brain Research*, *147*, 249–262. https://doi.org/10.1016/S0079-6123(04)47019-8, PubMed: 15581711

van Bergen, R. S., Ma, W. J., Pratte, M. S., & Jehee, J. F. M. (2015). Sensory uncertainty decoded from visual cortex predicts behavior. *Nature Neuroscience*, *18*, 1728–1730. https://doi.org/10.1038/nn.4150, PubMed: 26502262

Vo, V. A., Sprague, T. C., & Serences, J. T. (2017). Spatial tuning shifts increase the discriminability and fidelity of population codes in visual cortex. *Journal of Neuroscience*, *37*, 3386–3401. https://doi.org/10.1523/JNEUROSCI.3484-16.2017, PubMed: 28242794

Wallis, J. D., Anderson, K. C., & Miller, E. K. (2001). Single neurons in prefrontal cortex encode abstract rules. *Nature*, *411*, 953–956. https://doi.org/10.1038/35082081, PubMed: 11418860

Wallis, J. D., & Miller, E. K. (2003). Neuronal activity in primate dorsolateral and orbital prefrontal cortex during performance of a reward preference task. *European Journal of Neuroscience*, *18*, 2069–2081. https://doi.org/10.1046/j.1460-9568.2003.02922.x, PubMed: 14622240

Wandell, B. A., Dumoulin, S. O., & Brewer, A. A. (2007). Visual field maps in human cortex. *Neuron*, *56*, 366–383. https://doi.org/10.1016/j.neuron.2007.10.012, PubMed: 17964252

Warden, M. R., & Miller, E. K. (2010). Task-dependent changes in short-term memory in the prefrontal cortex. *Journal of Neuroscience*, *30*, 15801–15810. https://doi.org/10.1523/JNEUROSCI.1569-10.2010, PubMed: 21106819

White, I. M., & Wise, S. P. (1999). Rule-dependent neuronal activity in the prefrontal cortex. *Experimental Brain Research*, *126*, 315–335. https://doi.org/10.1007/s002210050740, PubMed: 10382618

Williams, D. W., & Sekuler, R. (1984). Coherent global motion percepts from stochastic local motions. *Vision Research*, *24*, 55–62. https://doi.org/10.1016/0042-6989(84)90144-5, PubMed: 6695508

Xu, J., Moeller, S., Auerbach, E. J., Strupp, J., Smith, S. M., Feinberg, D. A., et al. (2013). Evaluation of slice accelerations using multiband echo planar imaging at 3 T. *Neuroimage*, *83*, 991–1001. https://doi.org/10.1016/j.neuroimage.2013.07.055, PubMed: 23899722

Yoo, A. H., Klyszejko, Z., Curtis, C. E., & Ma, W. J. (2018). Strategic allocation of working memory resource. *Scientific Reports*, *8*, 16162. https://doi.org/10.1038/s41598-018-34282-1, PubMed: 30385803

Yu, Q., Teng, C., & Postle, B. R. (2020). Different states of priority recruit different neural representations in visual working memory. *PLoS Biology*, *18*, e3000769. https://doi.org/10.1371/journal.pbio.3000769, PubMed: 32598358

Zemel, R. S., Dayan, P., & Pouget, A. (1998). Probabilistic interpretation of population codes. *Neural Computation*, *10*, 403–430. https://doi.org/10.1162/089976698300017818, PubMed: 9472488